1

CASE FILE
COPY

NACA TN 2753

NATIONAL ADVISORY COMMITTEE FOR AERONAUTICS

TECHNICAL NOTE 2753

EFFECTS OF MACH NUMBER VARIATION BETWEEN 0.07 AND 0.34 AND REYNOLDS NUMBER VARIATION BETWEEN 0.97×10^6 AND 8.10×10^6 ON THE MAXIMUM LIFT COEFFICIENT OF A WING OF NACA 64-210 AIRFOIL SECTIONS

By James E. Fitzpatrick and William C. Schneider

Langley Aeronautical Laboratory
Langley Field, Va.

NACA
Washington
August 1952

1U

NATIONAL ADVISORY COMMITTEE FOR AERONAUTICS

TECHNICAL NOTE 2753

EFFECTS OF MACH NUMBER VARIATION BETWEEN 0.07 AND 0.34 AND REYNOLDS NUMBER VARIATION BETWEEN 0.97×10^6 AND 8.10×10^6 ON THE MAXIMUM LIFT COEFFICIENT OF A WING OF NACA 64-210 AIRFOIL SECTIONS

By James E. Fitzpatrick and William C. Schneider

SUMMARY

The effects of Mach number and Reynolds number on the maximum lift coefficient of a wing of NACA 64-210 airfoil sections are presented. The wing was tested through the speed range of the Langley 19-foot pressure tunnel at two values of air pressure. The ranges of Mach number obtained were from 0.07 to 0.34 at atmospheric pressure and from 0.08 to 0.26 at a pressure of 33 pounds per square inch absolute. The corresponding Reynolds number ranges were from 0.97×10^6 to 4.44×10^6 and from 2.20×10^6 to 8.10×10^6, respectively. The tests were made with and without partial-span and full-span split flaps deflected 60°. Pressure-distribution measurements were obtained for all configurations.

The maximum lift coefficient was a function of the two independent variables, Mach number and Reynolds number, and both parameters had an important effect on the maximum lift coefficient in the ranges investigated. The stall-progression and, consequently, the shape of the lift-curve at the stall were influenced by variations in both Mach number and Reynolds number. Peak maximum lift coefficients were measured at Mach numbers between 0.12 and 0.20, depending on the Reynolds number range and flap configuration.

There was very little influence of either Mach number or Reynolds number on the maximum lift of the wing with leading-edge roughness.

INTRODUCTION

The maximum lift of airfoils as influenced by Reynolds number has received extensive treatment (for example, ref. 1). Relatively little consideration, however, has been given to the interrelated influence

of compressibility and Reynolds number on the maximum lift. These interrelated effects were shown to be significant at Mach numbers as low as 0.2 in references 2 and 3. An investigation has been conducted, therefore, to study qualitatively these interrelated effects of compressibility and Reynolds number.

Three wings, differing only in airfoil sections, have been tested in both the Langley 19-foot pressure tunnel and the Langley 16-foot high-speed tunnel. The tests in the 19-foot pressure tunnel were conducted with the test air at atmospheric pressure and at a pressure of 33 pounds per square inch absolute. Two variations of Mach number with Reynolds number were thus obtained. The tests in the 16-foot tunnel (refs. 4 to 7) were conducted up to a Mach number of about 0.65 and were primarily concerned with the effect of compressibility on the maximum lift and loading. Results of the investigations in the 19-foot pressure tunnel of the wings of NACA 230-series airfoil sections and of NACA 66-series airfoil sections have been reported in references 8 and 9, respectively.

The present paper contains the results of the investigation of the wing of NACA 64-210 airfoil sections in the Langley 19-foot pressure tunnel. This wing was tested through a Mach number range from 0.07 to 0.34 at atmospheric pressure and from 0.08 to 0.26 at a pressure of 33 pounds per square inch. The corresponding Reynolds number ranges were from 0.97×10^6 to 4.44×10^6 and from 2.20×10^6 to 8.10×10^6, respectively. The investigation included force measurements and surface pressure-distribution measurements at six spanwise stations. The tests were made with and without partial-span and full-span split flaps deflected 60°. In addition, tests were made with leading-edge roughness for all conditions.

SYMBOLS

C_L	lift coefficient, $\text{Lift}/q_o S$
$C_{L_{max}}$	maximum lift coefficient
M_o	free-stream Mach number, U_o/a
M_l	local Mach number
P	pressure coefficient, $\frac{p - p_o}{q_o}$

P_{min}	minimum pressure coefficient measured on wing at $C_{L_{max}}$
R_o	free-stream Reynolds number, $\rho U_o \bar{c}/\mu$
$\bar{c}$	mean aerodynamic chord, $\frac{2}{S}\int_0^{b/2} c^2 dy$
u/U	ratio of local velocity inside boundary layer to velocity outside boundary layer
x/c	chordwise distance measured from leading edge, fraction of chord
z'/c	height perpendicular to wing surface, fraction of chord
s/c	surface distance from leading edge to center of orifice, fraction of chord
C	cross-sectional area of tunnel test section, sq ft
D	diameter of tunnel test section, ft
α	angle of attack of wing root chord, deg
α_{max}	angle of attack beyond which no appreciable lift increase occurs, deg
S	wing area, sq ft
U_o	free-stream velocity, ft/sec
a	speed of sound, ft/sec
b	wing span, ft
c	local chord, ft
p	local static pressure, lb/sq ft
p_o	free-stream static pressure, lb/sq ft
q_o	free-stream dynamic pressure, lb/sq ft

δ_w jet-boundary correction factor (ref. 10)

ρ mass density of air, slugs/cu ft

μ coefficient of viscosity of air, slugs/ft-sec

MODEL, APPARATUS, AND TESTS

Model and Apparatus

The plan form and principal dimensions of the wing are shown in figure 1. The wing has a span of 12 feet, an aspect ratio of 6, a washout of 1.5°, and a mean chord of 2 feet. The wing is composed of NACA 64-210 airfoil sections. Measurements of the airfoil ordinates showed the contour ahead of 10 percent of the chord to be correct to the true airfoil within 0.005 inch; the remainder of the contour was correct within 0.008 inch with few exceptions. The tips are semi-elliptical in cross section and begin at the 99-percent-semispan station. Because the wing was constructed of solid steel, the wing deflection was assumed to be negligible during the tests.

The split flaps had a chord of 20 percent of the local wing chord. The spans of the full-span and partial-span flaps were 99 percent and 55 percent of the wing span, respectively. Both types of flap were deflected 60° with the lower surface of the wing.

The leading-edge roughness consisted of No. 60 (0.011-in. mesh) carborundum grains applied across the complete span on a thin layer of shellac for a surface length of 8 percent chord measured from the leading edge on both upper and lower surfaces. The grains covered 5 to 10 percent of the affected area.

The model was mounted on a two-support system in the Langley 19-foot pressure tunnel (see fig. 2). The aerodynamic forces and moments were measured by a simultaneous-recording six-component balance.

The wing contained approximately 35 surface-pressure orifices at each of six spanwise stations. The spanwise location of the orifice stations is shown in figure 1, and the chordwise distribution of the pressure orifices is listed in table I. Additional orifices (table I) were installed during the investigation in order that the position and magnitude of the minimum pressure might be more accurately established. The pressure leads for the orifices originally installed in the model were conducted internally to a pipe protruding from the trailing edge at the plane of symmetry (fig. 1). They were then brought to multiple-tube manometers through a boom and a counterbalanced strut that moved

on vertical guides in a fairing (figs. 2 and 3). This system allowed continuous testing through the angle-of-attack range. This arrangement, however, did not allow reliable force tests to be made simultaneously with pressure measurements; consequently, force tests were made with the tube-transfer system removed. During the force tests a short fairing cap (fig. 1) covered the pipe extending from the trailing edge at the plane of symmetry.

For the orifices added during the tests, the pressure leads were conducted along the lower surface (fig. 2) and down the support strut to the multiple-tube manometer. The leads for the additional orifices were brought out of the wing sufficiently far behind the leading edge on the lower surface so as not to interfere with the minimum peak measurement on the upper surface.

Tests

Tests were conducted at tunnel pressures of 14.7 and 33 pounds per square inch absolute. The ranges of Mach number and Reynolds number thus obtained were as follows:

Tunnel pressure, lb/sq in. abs.	Mach number range	Reynolds number range
14.7	0.07 to 0.34	0.97×10^6 to 4.44×10^6
33	.08 to .26	2.20×10^6 to 8.10×10^6

The variations of Mach number with Reynolds number for these two pressures are shown in figure 4 for the present tests.

Force tests with the wing both smooth and rough were made through the speed range at both tunnel pressures. Chordwise pressure-distribution measurements were made at both tunnel pressures for values of the Mach number corresponding to those of the force tests. Some measurements of the pressure fluctuation were made at $C_{l_{max}}$ for Mach numbers of 0.14, 0.19, and 0.20 with an NACA high-response pressure cell located at the 0.4-semispan station for an x/c of 0.001. These measurements were obtained at a pressure of 33 pounds per square inch.

Pressure-distribution tests were also made with roughness on the leading edge. Some measurements of the boundary layer were made to determine the effects of Mach number on turbulent-boundary-layer thickness and shape. Visual observations of the stalling pattern were

made by means of tuft studies at several tunnel airspeeds. The wing was tested through an angle-of-attack range from -6.5° through the stall.

The data were obtained with the air in the tunnel at condensation-free conditions. Conditions for no condensation were determined as a relationship between dew point and stagnation temperature from unpublished calculations based on nuclei-formation theory (Lewis Laboratory). When these conditions were maintained, the data were repeatable.

CORRECTIONS TO DATA

Force Tests

The lift coefficients have been corrected for support-strut tare and interference as determined by tare tests with an image support system.

The angles of attack have been corrected for air-stream misalinement and jet-boundary effects. The air-stream misalinement was determined during the tare tests; however, jet-boundary correction was determined by the following equation derived from reference 10:

$$\Delta\alpha = \left(1 + \frac{1.05\bar{c}}{D\sqrt{1 - M_o^2}}\right)\delta_w \frac{S}{C} 57.3C_L$$

This equation contains the angle-of-attack correction at the lifting line for a wing with an elliptical spanwise load distribution and also an additional correction for the induced streamline curvature. The term $\sqrt{1 - M_o^2}$ has been introduced to account for compressibility effects (ref. 11). For the tests in the Langley 19-foot pressure tunnel, an average value of $\sqrt{1 - M_o^2}$ was found to suffice and the total correction to the angle of attack becomes $0.678C_L$.

Pressure-Distribution Tests

No corrections have been applied to the local values of static pressure. The orifice stations were selected so that the local effects of the struts on these pressures could be assumed negligible. In the computation of the pressure coefficients, average free-stream dynamic

pressure and average free-stream static pressure across the span have been used, inasmuch as tunnel surveys indicate these pressures to be constant within 1.5 percent of the free-stream dynamic pressure over the survey stations.

RESULTS AND DISCUSSION

Observations of Data

The basic lift data of the wing in both the smooth and rough conditions are presented in figures 5, 6, and 7 for the Mach number and Reynolds number ranges shown in figure 4. The maximum lift coefficients and the angles of attack for maximum lift from these lift curves are plotted against free-stream Mach number and free-stream Reynolds number in figures 8 and 9, together with the minimum pressure coefficients for the same conditions.

Lift characteristics of smooth wing.- The effect of Reynolds number on the lift characteristics of the smooth wing may be seen by comparing the value of $C_{L_{max}}$ at a constant Mach number at both tunnel pressures (fig. 8). The effect of an increase in Reynolds number at constant Mach number is seen on the plot of $C_{L_{max}}$ against Mach number by following a vertical line (fig. 8(a)) from the lower curve (atmospheric pressure) to the upper curve (pressure, 33 lb/sq in.) For example, increasing the Reynolds number from 1.44×10^6 (point A) to 3.15×10^6 (point B) at a Mach number of 0.10 increases $C_{L_{max}}$ from 0.950 to 1.385. The effect of Mach number can be seen by comparing the value of $C_{L_{max}}$ at a constant Reynolds number for both tunnel pressures. For example, at a Reynolds number of 3.15×10^6 (fig. 8(a)), the maximum lift coefficient at a pressure of 33 pounds per square inch (M = 0.10, point B) is 1.385, and at atmospheric pressure (M = 0.22, point C) it is 1.020. This reduction is accompanied by a similar reduction in angle of attack for maximum lift. Perhaps the most important conclusion to be drawn from figure 8 is that the effect of Reynolds number on the maximum lift coefficient depends upon the Mach number and, conversely, the effect of Mach number depends upon the Reynolds number, as previously demonstrated in reference 9. It should be pointed out that such a large effect of Mach number on maximum lift was not obtained in the unpublished data on the two-dimensional model of the same airfoil in the Langly low-turbulence pressure tunnel through the same Mach and Reynolds number ranges. The full explanation of this difference, however, is not known.

Stall progressions.- The relative effect of Mach and Reynolds numbers on the stall progression is indicated by the lift curves presented

in figures 5, 6, and 7 and by the stall patterns (fig. 10) sketched from tuft observations. The lift curves obtained from the tests at atmospheric pressure (figs. 5(a), 6(a), and 7(a)) have rounded tops; whereas, those from tests at a pressure of 33 pounds per square inch (figs. 5(b), 6(b), and 7(b)) have sudden breaks at $C_{L_{max}}$ except for the highest Mach numbers. At a pressure of 33 pounds per square inch, the stall becomes less abrupt and the stalled area more localized as the Mach number increases beyond that for peak $C_{L_{max}}$. The round-top lift curves, such as those obtained in the tests at atmospheric pressure, are characterized in this case by a lower value of $C_{L_{max}}$ and are associated with a gradual stall progression starting near the trailing edge at the midsemispan and spreading forward and inboard (fig. 10). This type of stall progression is also apparent at the high Mach number (0.25) in the tests at a pressure of 33 pounds per square inch.

The stall progression and, consequently, the shape of the lift curve at the stall depend upon both Mach number and Reynolds number. The Mach number at which the change from an abrupt to a gradual stall progression occurs depends on the Reynolds number range. For example, in the high Reynolds number range (tests at a pressure of 33 lb/sq in., fig. 5(b)) the change occurs at about $M_o = 0.25$; whereas, in the low Reynolds number range (atmospheric pressure, fig. 5(a)) the stall is not abrupt throughout the Reynolds number range of the present tests. Conversely, the Reynolds number at which the abrupt stall begins depends on the Mach number range. For example, in the low Mach number range (tests at a pressure of 33 lb/sq in., fig. 5(b)) the stall becomes abrupt at Reynolds numbers somewhat less than 2.50×10^6; whereas, in the high Mach number range (tests at atmospheric pressure, fig. 5(a)) it remains gradual even at Reynolds numbers of 4.00×10^6.

Interrelated effects.- As previously pointed out, the maximum lift is a function of two independent variables, Mach number and Reynolds number. An increase in Mach number tends to decrease $C_{L_{max}}$, and an increase in Reynolds number tends to increase $C_{L_{max}}$. On the basis of data from present and previous investigations, the important influences of local Mach number can be qualitatively emphasized by the following considerations. The adverse Mach number effect appears greater at the higher Reynolds numbers because the effect of Reynolds number is to maintain attached flow to higher angles of attack, so that high local velocities exist around the nose. As can be seen from figure 11, if an airfoil were tested through a Mach number range at a constant low value of Reynolds number and if there were no adverse Mach number effect, the minimum pressure coefficient would travel from A to D'. If there were an adverse Mach number effect, the minimum pressure coefficient

would travel from A to D. Through the same Mach number range, but at a higher constant Reynolds number, the minimum pressure coefficient would go from B to C. The decrement in pressure coefficient, through the same Mach number range, is larger at the higher Reynolds number.

Through a Reynolds number range at a constant low Mach number, if there were no Mach number effect, the minimum pressure coefficient would travel from A to B'. Since there is a Mach number effect, the variation is from A to B. Through the same Reynolds number range, but at a higher constant Mach number, the variation is from D to C which is much shorter than from A to B. The beneficial effect of Reynolds number is thus reduced to a greater extent at the higher Mach number because of the influence of Mach number on the Reynolds number effect. In any variation of minimum pressure coefficient with airspeed, therefore, the mutual interdependence of the Reynolds number effect and Mach number effect is in evidence. Although figure 11 describes the minimum pressure coefficient, a parallel case might be drawn for the maximum lift coefficient.

Effect of roughness.- Very little change occurred in the maximum lift coefficient of the wing with the leading-edge roughness through the Reynolds number and Mach number range for any configuration (fig. 9). The value of the maximum lift coefficient of the plain wing with roughness at both tunnel pressures was approximately the same as its value in the smooth condition at atmospheric pressure at Reynolds numbers above 2.40×10^6. The peak minimum pressure coefficients were reduced by roughness by about 30 percent in the tests at atmospheric pressure and by about 50 percent in the tests at a pressure of 33 pounds per square inch (compare figs. 8 and 9). Critical pressure coefficients were not obtained in the speed range of the present tests, but an increase in Mach number slightly reduced the maximum lift coefficient and the peak negative pressure coefficient (fig. 9). The suction at practically all points was slightly reduced by roughness (fig. 12). A somewhat greater effect of Mach number and Reynolds number on the characteristics of the roughened wing was reported in reference 9.

Nature of Reynolds and Mach Number Effects

The importance of Reynolds and Mach numbers in affecting the maximum lift, as shown in the present investigation and those of references 8 and 9, suggests that a qualitative discussion of the possible physical nature of these effects may be of interest.

Reynolds number effects.- The manner in which the Reynolds number affects maximum lift is explained in reference 1 and is extended to include a wing of NACA 66-series airfoils in reference 9. As pointed out in that reference, airfoils are characterized at low Mach numbers and Reynolds numbers by separation of the laminar boundary layer just downstream of the minimum pressure point (ref. 12). Several investigations have shown (for example, refs. 1 and 12) that, if the Reynolds number is sufficiently high, the separated flow will reattach to the airfoil surface at a point downstream of the separation point as a

turbulent boundary layer. The point of reattachment moves upstream with increasing Reynolds number. The enclosed region of separated flow is called a separation bubble.

Reynolds number has a negligible effect on the maximum lift coefficient below the Reynolds number at which a separation bubble forms. A further increase in Reynolds number will diminish the size of the bubble, and the following two effects may be apparent: The point of reattachment of the flow moves forward, and a greater extent of turbulent boundary layer, which is more resistant to separation, results over the rear portion of the airfoil (ref. 1). Higher angles of attack and accompanying increases in maximum lift coefficient are consequently obtained before flow breakdown. At a sufficiently high Reynolds number, the separation bubble is finally eliminated, and the transition moves toward the position of minimum pressure. As shown in reference 1, the maximum lift coefficient would not be expected to increase with a further increase in Reynolds number.

Mach number effects, subcritical range.- The Prandtl-Glauert approximation indicates that an increase in Mach number in the subcritical range effects a greater pressure minimum at the higher Mach number. At any angle of attack below the stall, therefore, a higher lift coefficient results. Figure 13(a) shows, by way of illustration, a small negative increment in minimum pressure coefficient as the Mach number is increased from 0.10 to 0.22 at approximately the same Reynolds number. (Of course, the negative increment is very small since the Mach number increment of only 0.12 occurs in a range of shallow pressure-coefficient rise with Mach number.) If the maximum lift were dependent solely on the pressure recovery and Reynolds number, similar values of maximum lift might therefore be expected at both Mach numbers with a slight reduction in the stalling angle. Actually, however, the stalling angle is markedly reduced and the same maximum-lift pressure recovery is not obtained at both Mach numbers (fig. 13(b)). Since the Reynolds number is nearly constant, the boundary-layer separation which restricts $C_{L_{max}}$, α_{max}, and P_{min} is, in all probability, influenced in some manner by the Mach number. In this Mach number range, compressibility does not seem to affect the turbulent-boundary-layer thickness or shape, as shown by the boundary-layer measurements presented in figure 14. It may then be reasonable to expect that the Mach number effect is associated with the laminar boundary layer near the leading edge and/or the formation and behavior of the laminar separation bubble.

An indication of at least one compressibility effect is provided by theoretical considerations. For example, in a velocity field corresponding to that over an airfoil, an increase in local-stream Mach number tends to decrease the velocity in the inner one-third of the boundary layer and to increase it in the remainder. This tendency leads

to a forward movement of the laminar separation point as compared with its position for the incompressible case. When this result is applied to the present investigation, in the low Reynolds number range, an increase in Mach number at a given Reynolds number results in the occurrence of laminar separation at a smaller radius of curvature on the airfoil nose. If the return angle is assumed to be constant, the point of reattachment is extended downstream so that a thicker, more unstable turbulent boundary layer results.

A comparison of figure 8 with the similar figures of references 8 and 9 at the same conditions of free-stream Mach and Reynolds numbers shows a greater subcritical P_{min} for the present wing, an indication of greater accelerations around the sharper nose, and higher local Mach numbers outside the boundary layer. Because the present wing exhibits higher local velocities at maximum lift, the greater effect of Mach number might be expected.

Mach number effects, supercritical range.- The results of references 8 and 9 indicate that an abrupt reduction in $C_{L_{max}}$ occurs when the critical Mach number is first attained at some point on the wing. Presumably a slight shock resulted which, at the critical conditions of maximum lift, precipitated a stall. As can be seen from figure 8, the peak maximum lift coefficients were measured at Mach numbers between 0.12 and 0.20, depending upon the flap configuration and Reynolds number range. In the present tests at a pressure of 33 pounds per square inch, the abrupt reduction was not coincident with the attainment of local sonic speed. This result may have been because no shock occurred; but in order to judge the present data, consideration must be given the orifice distribution. The location of an orifice at the exact position of peak pressure for all conditions is unlikely because of the high-pressure gradients around the airfoil nose (figs. 13 and 15). The pressure fluctuations, not recordable by a photograph of the manometer, must also be considered. The pressure coefficients measured with the NACA high-response pressure cell at maximum lift were found to fluctuate 4.8, 6.7, and 8.8 percent at Mach numbers of 0.14, 0.19, and 0.20, respectively. Although the pressure-cell orifice was not located at the precise position of minimum pressure, these percentages have been applied to the minimum pressure coefficients measured and are designated by flagged symbols in figure 8. At a pressure of 33 pounds per square inch, then, the abrupt reduction in $C_{L_{max}}$ of the wing may have been coincident with the attainment of sonic speed somewhere on the wing. As the Mach number is further increased, the critical pressure coefficient was reached at lower angles of attack and, as a result, the maximum lift coefficient was reduced considerably. The magnitude of this reduction can be obtained from figure 8. When the results obtained at atmospheric pressure are compared with those obtained at a pressure of 33 pounds per square inch at a constant Reynolds number, a change in Mach number reduces

the maximum lift coefficient. For example, at a Reynolds number of 4.50×10^6 a change in Mach number from 0.135 to 0.320 reduces $C_{L_{max}}$ from 1.44 to 1.03. Figure 8(a) also shows that the minimum pressure coefficient measured under the same conditions at a Mach number of 0.135 was subcritical and at a Mach number of 0.320 was supercritical. Similar results were obtained for the configurations with flaps (figs. 8(b) and 8(c)).

SUMMARY OF RESULTS

The results of the investigation of the wing of NACA 64-210 airfoil sections in the Langley 19-foot pressure tunnel may be summarized as follows:

1. The maximum lift coefficient was a function of the two independent variables, Mach number and Reynolds number, and both parameters had an important effect on the maximum lift in the ranges investigated.

2. The stall-progression and, consequently, the shape of the lift curve at the stall were influenced by variations in both Mach number and Reynolds number.

3. Peak maximum lift coefficients were measured at Mach numbers between 0.12 and 0.20, depending upon the flap configuration and Reynolds number range.

4. There was very little influence of either Mach number or Reynolds number on the maximum lift of the wing with leading-edge roughness. The value of the maximum lift coefficient of the plain wing with roughness at both tunnel pressures was approximately the same as its value in the smooth condition at atmospheric pressure at Reynolds numbers above 2.40×10^6. The reduction in maximum lift caused by roughness was associated with a 30- to 50-percent reduction in leading-edge suction peaks and a slight reduction in suction elsewhere over the surface.

Langley Aeronautical Laboratory,
National Advisory Committee for Aeronautics,
Langley Field, Va., April 8, 1952.

REFERENCES

1. Jacobs, Eastman N., and Sherman, Albert: Airfoil Section Characteristics As Affected by Variations of the Reynolds Number. NACA Rep. 586, 1937.

2. Muse, Thomas C.: Some Effects of Reynolds and Mach Numbers on the Lift of an NACA 0012 Rectangular Wing in the NACA 19-Foot Pressure Tunnel. NACA CB 3E29, 1943.

3. Stack, John, Fedziuk, Henry A., and Cleary, Harold E.: Preliminary Investigation of the Effect of Compressibility on the Maximum Lift Coefficient. NACA ACR, Feb. 1943.

4. Pearson, E. O., Jr.: Effect of Compressibility on the Distribution of Pressures Over a Tapered Wing of NACA 230-Series Airfoil Sections. NACA TN 1390, 1947.

5. Cooper, Morton, and Korycinski, Peter F.: The Effects of Compressibility on the Lift, Pressure, and Load Characteristics of a Tapered Wing of NACA 66-Series Airfoil Sections. NACA TN 1697, 1948.

6. West, F. E., Jr., and Hallissey, J. M., Jr.: Effects of Compressibility on Normal-Force, Pressure, and Load Characteristics of a Tapered Wing of NACA 66-Series Airfoil Sections With Split Flaps. NACA TN 1759, 1948.

7. West, F. E., Jr., and Himka, T.: Effects of Compressibility on Lift and Load Characteristics of a Tapered Wing of NACA 64-210 Airfoil Sections up to a Mach Number of 0.60. NACA TN 1877, 1949.

8. Furlong, G. Chester, and Fitzpatrick, James E.: Effects of Mach Number and Reynolds Number on the Maximum Lift Coefficient of a Wing of NACA 230-Series Airfoil Sections. NACA TN 1299, 1947.

9. Furlong, G. Chester, and Fitzpatrick, James E.: Effects of Mach Number up to 0.34 and Reynolds Number up to 8×10^6 on the Maximum Lift Coefficient of a Wing of NACA 66-Series Airfoil Sections. NACA TN 2251, 1950.

10. Silverstein, Abe, and White, James A.: Wind-Tunnel Interference With Particular Reference to Off-Center Positions of the Wing and to the Downwash at the Tail. NACA Rep. 547, 1936.

11. Goldstein, S., and Young, A. D.: The Linear Perturbation Theory of Compressible Flow, With Applications to Wind-Tunnel Interference. R. & M. No. 1909, British A.R.C., 1943.

12. Von Doenhoff, Albert E., and Tetervin, Neal: Investigation of the Variation of Lift Coefficient With Reynolds Number at a Moderate Angle of Attack on a Low-Drag Airfoil. NACA CB, Nov. 1942.

TABLE I.- CHORDWISE ORIFICE LOCATIONS

x/c		x/c		x/c	
Upper	Lower	Upper	Lower	Upper	Lower
Station 1		Station 2		Station 2	
0(L.E.)	------	0(L.E.)	------	0(L.E.)	------
[a].0047	0.0125	[a].0021	0.0125	[a]0	0.0125
.0125	.0375	[a].0054	.0375	[a].00050	.0375
.0375	.0625	.0125	.0625	[a].00054	.0625
.0625	.0875	.0375	.0875	[a].00354	.125
.0875	.125	.0625	.125	[a b].0083	.175
.125	.175	.0875	.175	.0125	.225
.175	.225	.125	.225	.0375	.325
.225	.325	.175	.325	.0625	.375
.275	.375	.225	.375	.0875	.425
.375	.475	.275	.425	.125	.550
.425	.550	.375	.475	.175	.650
.475	.650	.425	.550	.275	.750
.550	.750	.475	.650	.375	.850
.650	.850	.550	.750	.425	.950
.750	.950	.650	------	.475	------
.850	------	.750	------	.550	------
.950	------	.850	------	.650	------
------	------	.950	------	.750	------
------	------	------	------	.850	------
Station 4		Station 5		Station 6	
0(L.E.)	0.0125	0(L.E.)	0.0125	0(L.E.)	0.0125
[a].0036	.0375	[a].0036	.0375	.0125	.0375
[a].0077	.0625	[a].0091	.0625	.0375	.0625
.0125	.0875	.0125	.0875	.0625	.0875
.0375	.125	.0375	.175	.0875	.125
.0625	.225	.0625	.225	.125	.225
.0875	.275	.0875	.325	.175	.275
.125	.325	.125	.375	.225	.375
.175	.375	.175	.425	.275	.550
.225	.475	.225	.550	.325	.650
.275	.550	.275	.650	.375	.850
.375	.650	.375	.750	.475	.950
.425	.750	.425	.850	.550	------
.475	.950	.475	.950	.750	------
.550	------	.550	------	.950	------
.650	------	.650	------	------	------
.750	------	.750	------	------	------
.850	------	.850	------	------	------
.950	------	.950	------	------	------

[a]Additional orifices.

[b]This orifice location was substituted for orifice located at x/c of 0.00054 for some tests.

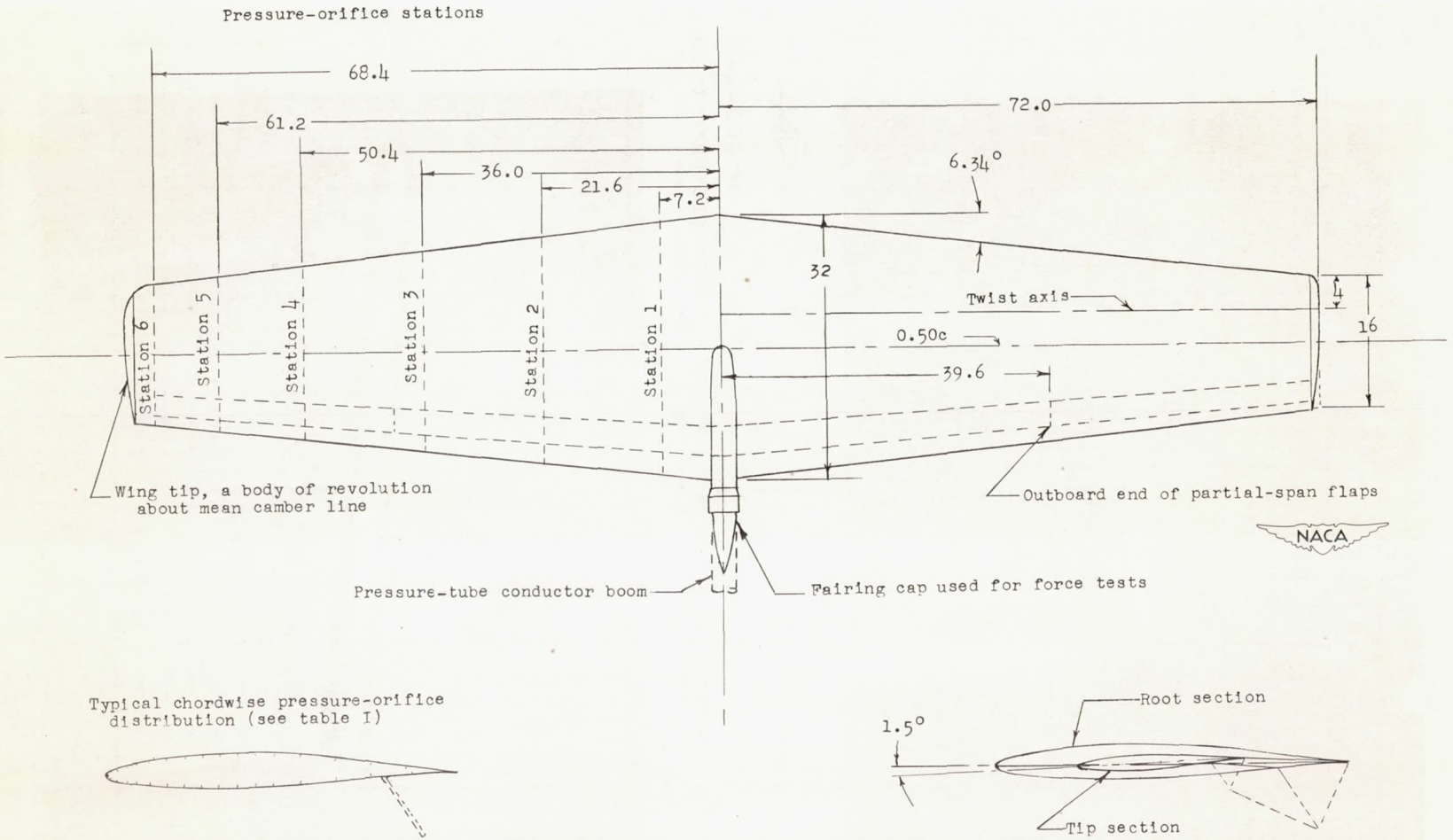
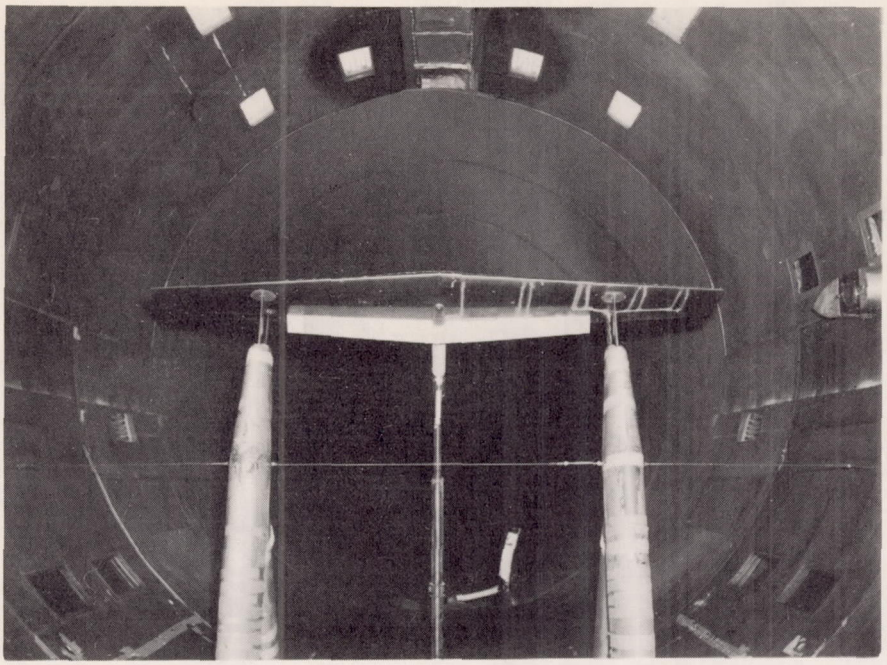


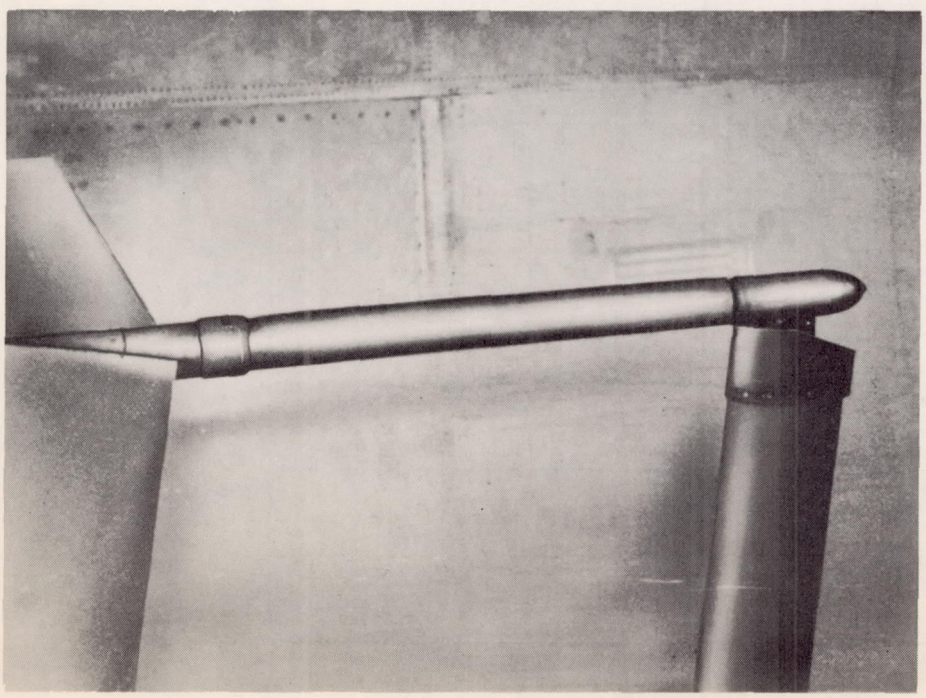
Figure 1.- Plan form and dimensions of wing of NACA 64-210 airfoil sections (all dimensions in inches). Aspect ratio, 6; taper ratio, 0.5; wing area, 24 square feet.



NACA

L-66304.1

Figure 2.- Test wing mounted in the Langley 19-foot pressure tunnel.



NACA

Figure 3.- Pressure-tube conductor system. L-45976.1

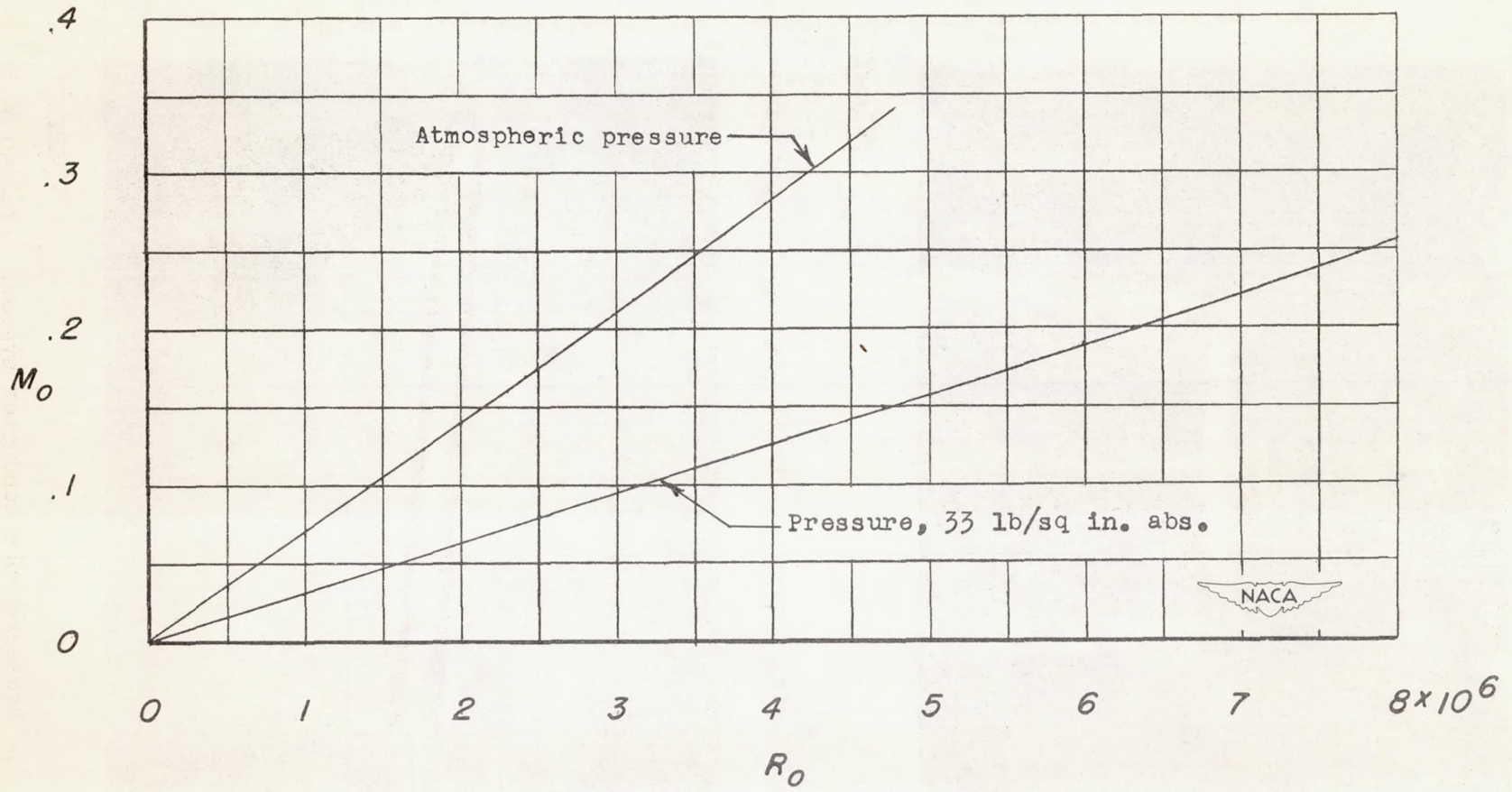
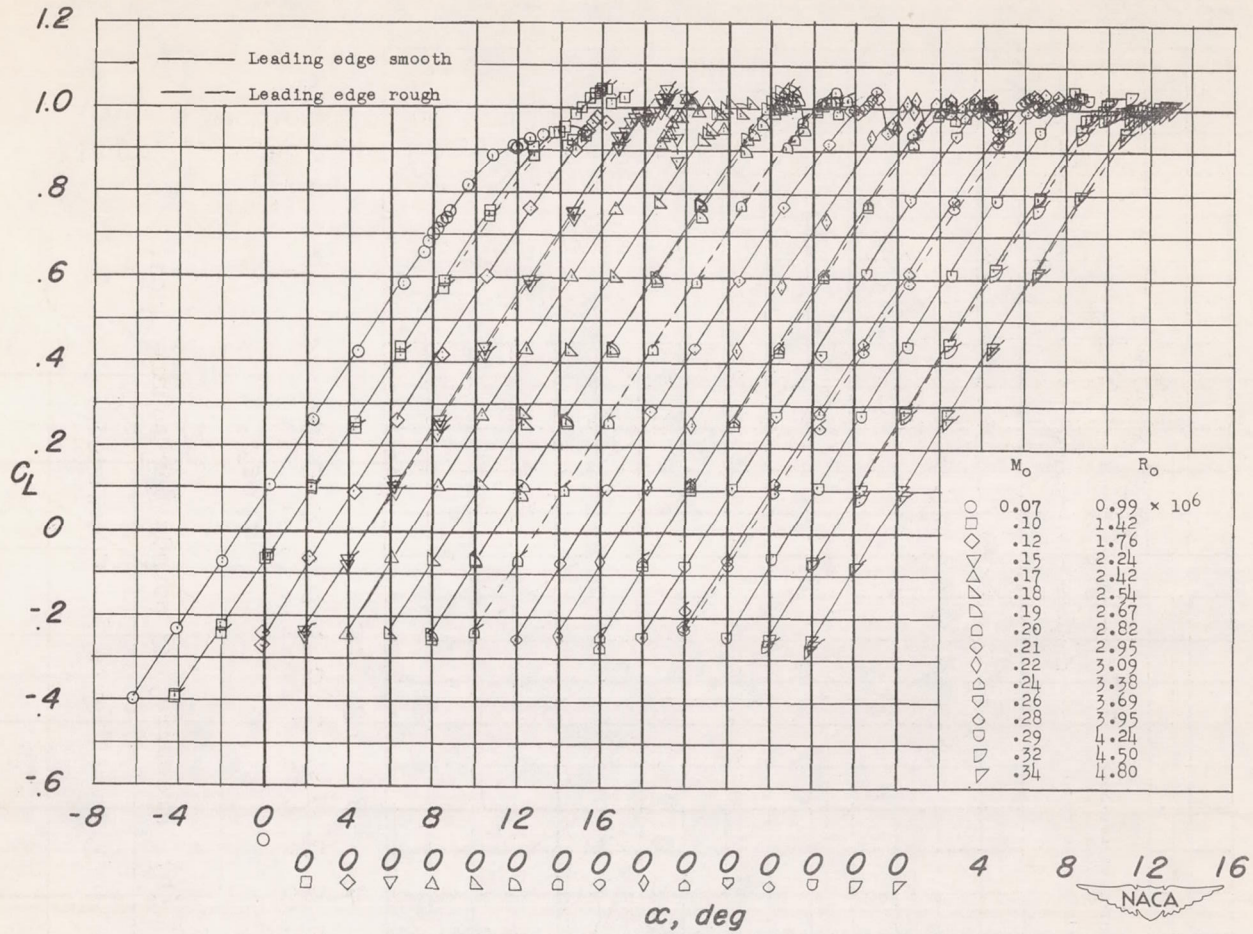
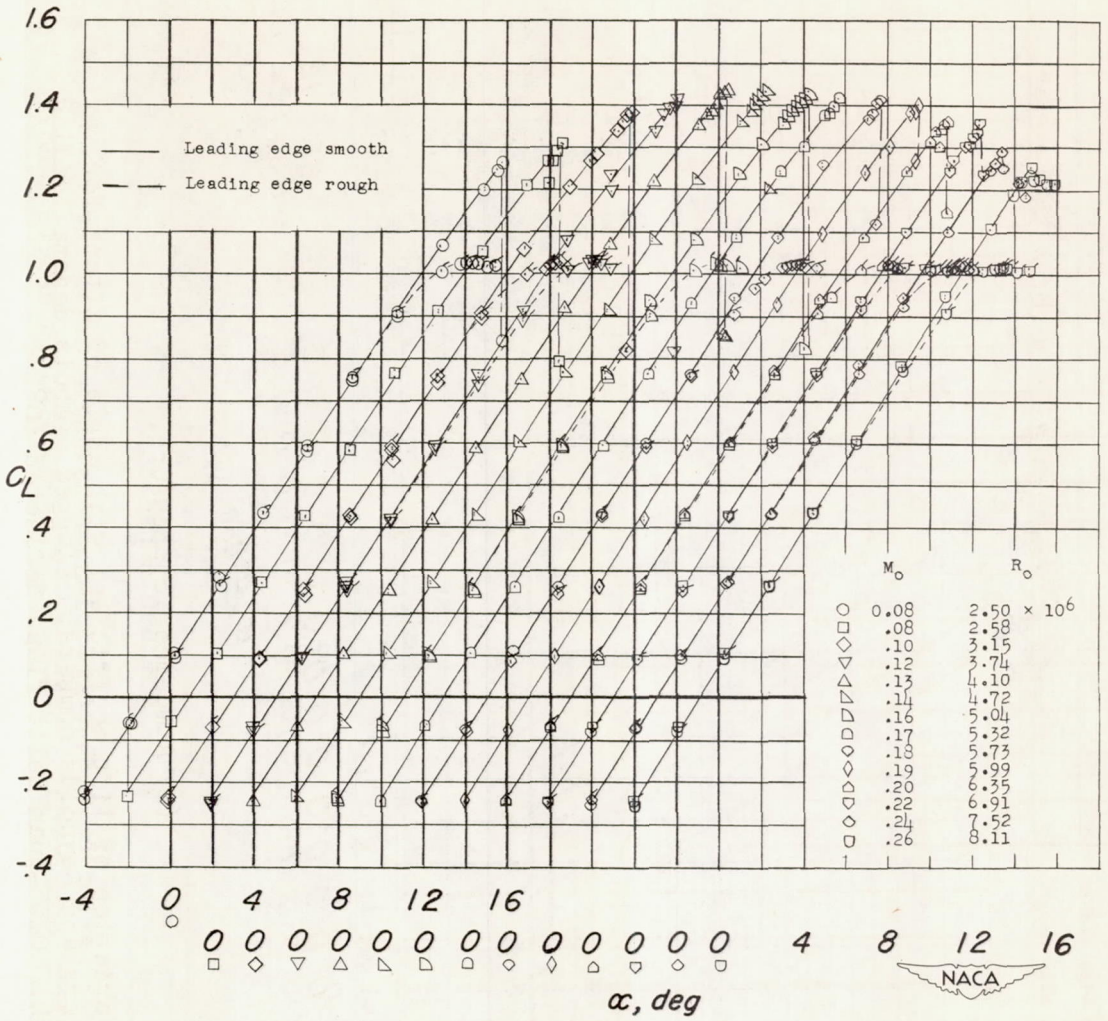


Figure 4.- Conditions for tests of the wing of NACA 64-210 airfoil sections in the Langley 19-foot pressure tunnel.



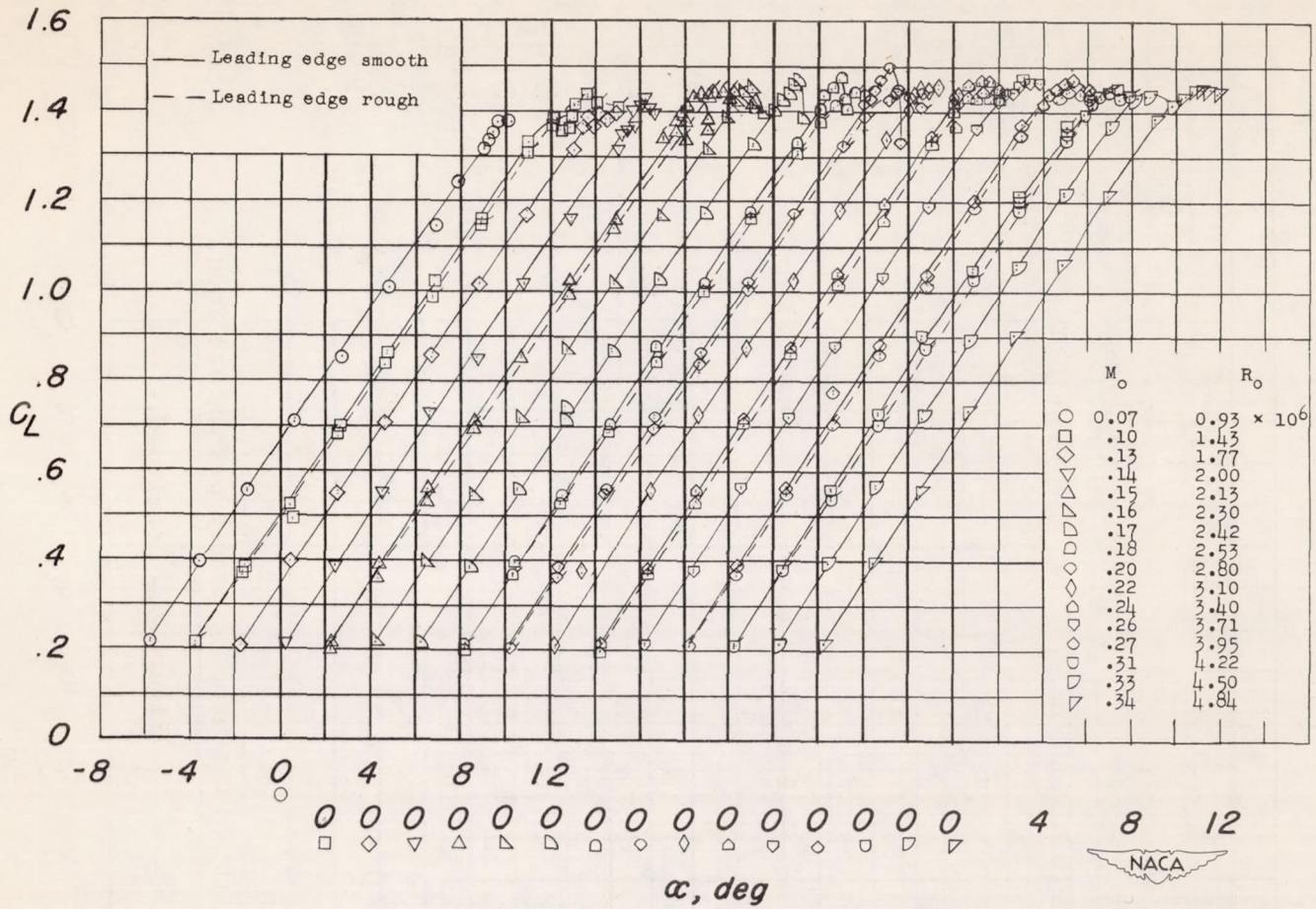
(a) Atmospheric pressure.

Figure 5.- Variation of lift coefficient with angle of attack for various Mach numbers and Reynolds numbers. Flagged symbols denote leading edge rough. Plain wing.



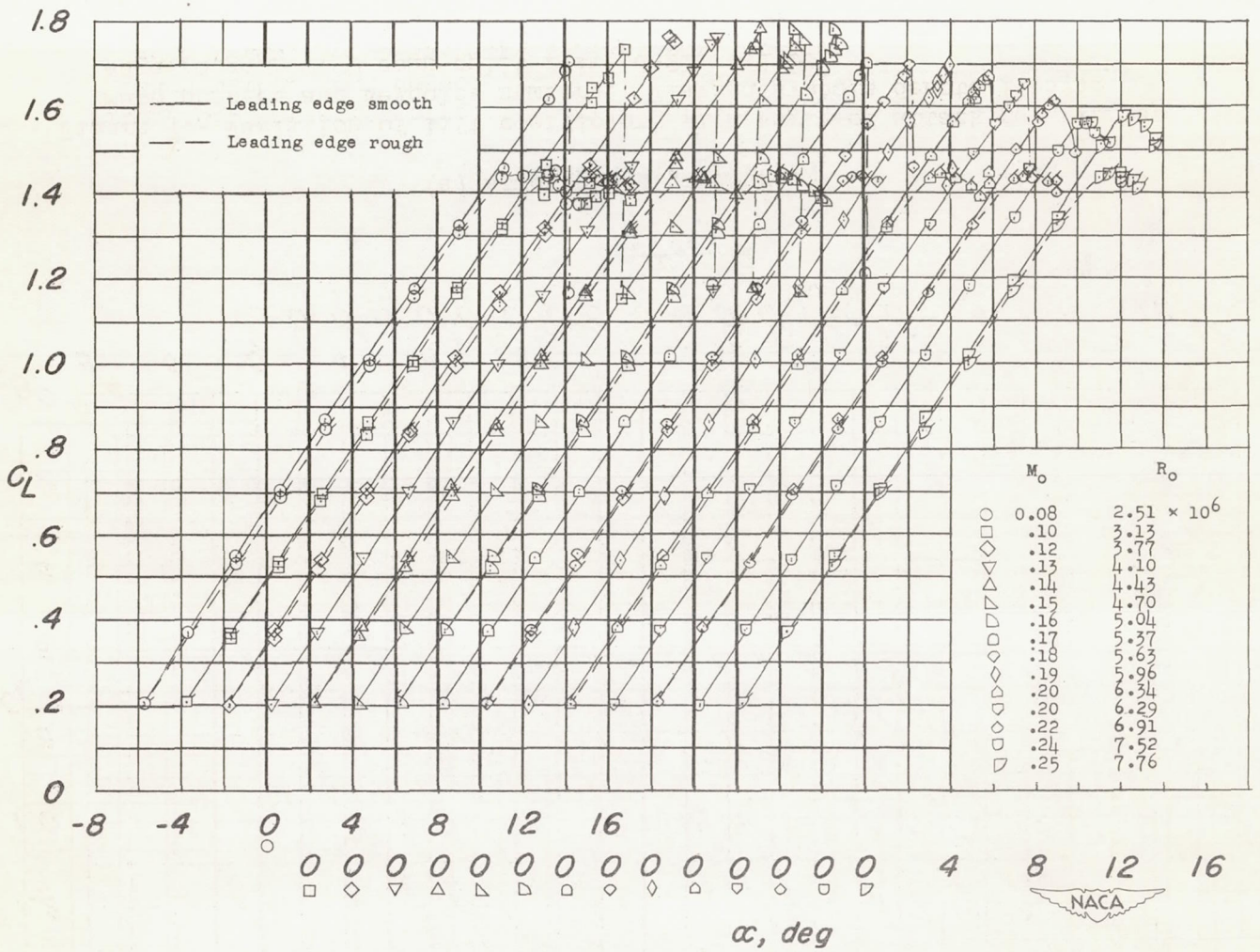
(b) Pressure, 33 pounds per square inch.

Figure 5.- Concluded.



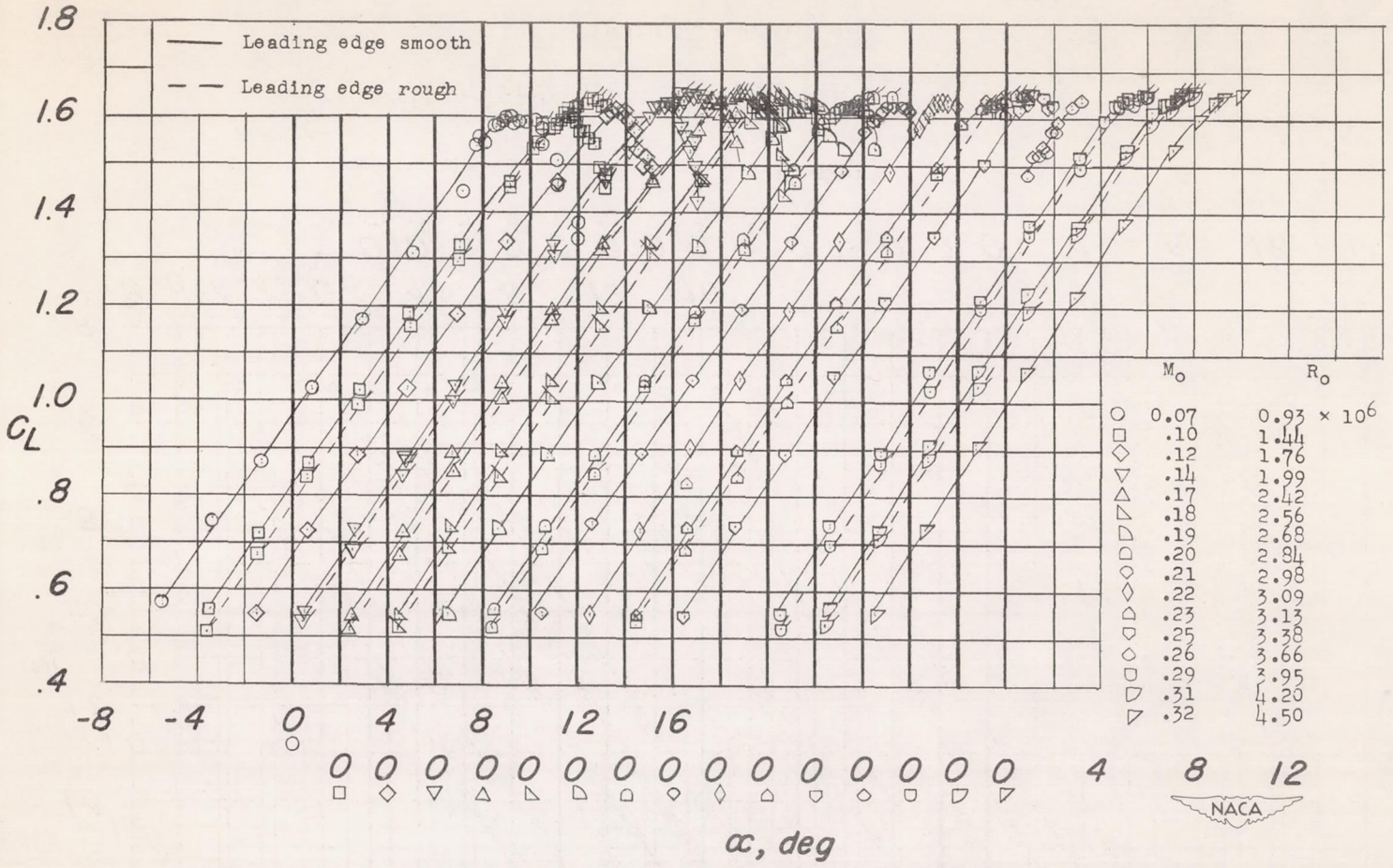
(a) Atmospheric pressure.

Figure 6.- Variation of lift coefficient with angle of attack for various Mach numbers and Reynolds numbers. Flagged symbols denote leading edge rough. 0.55-span split flaps deflected 60°.



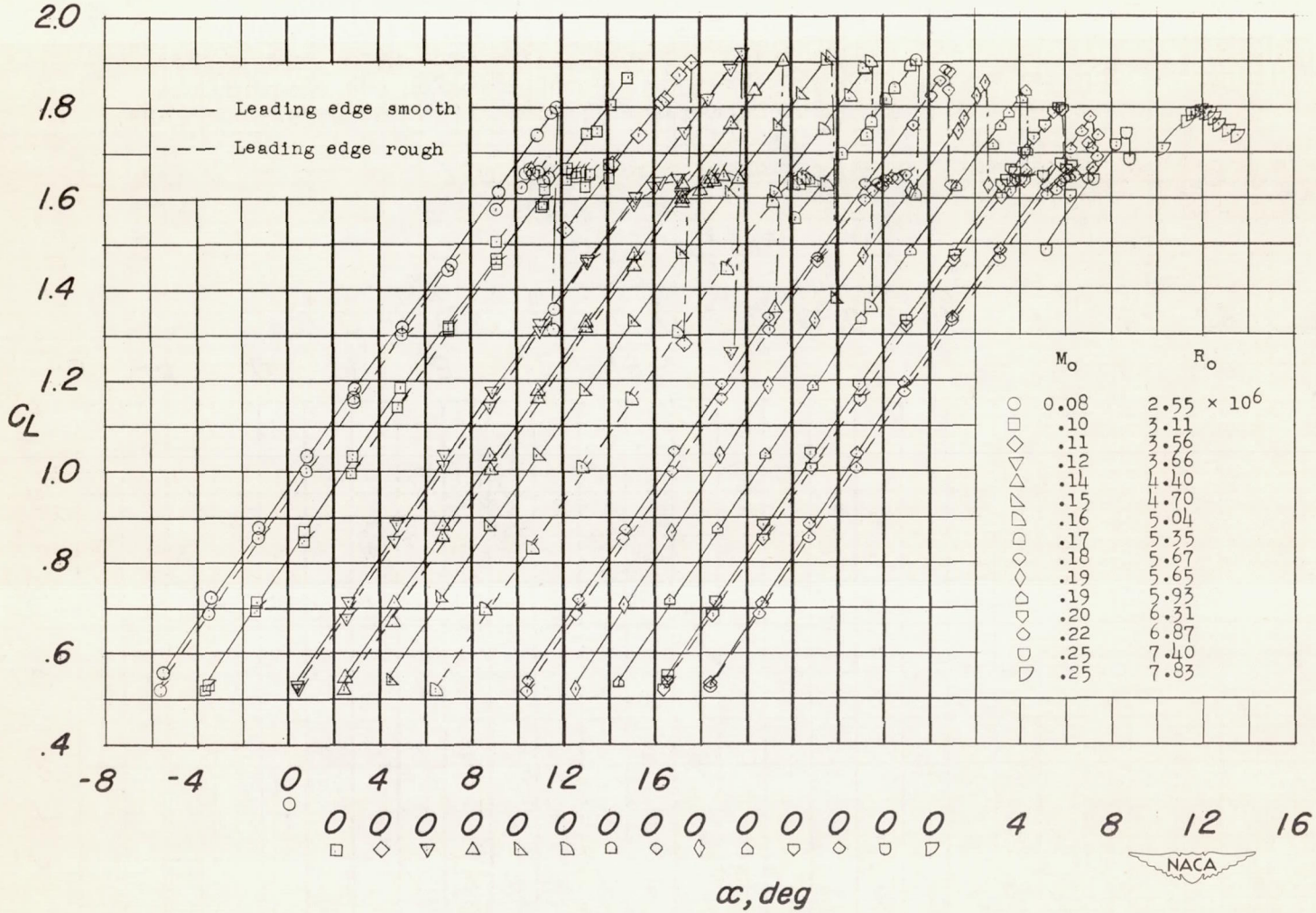
(b) Pressure, 33 pounds per square inch.

Figure 6.- Concluded.



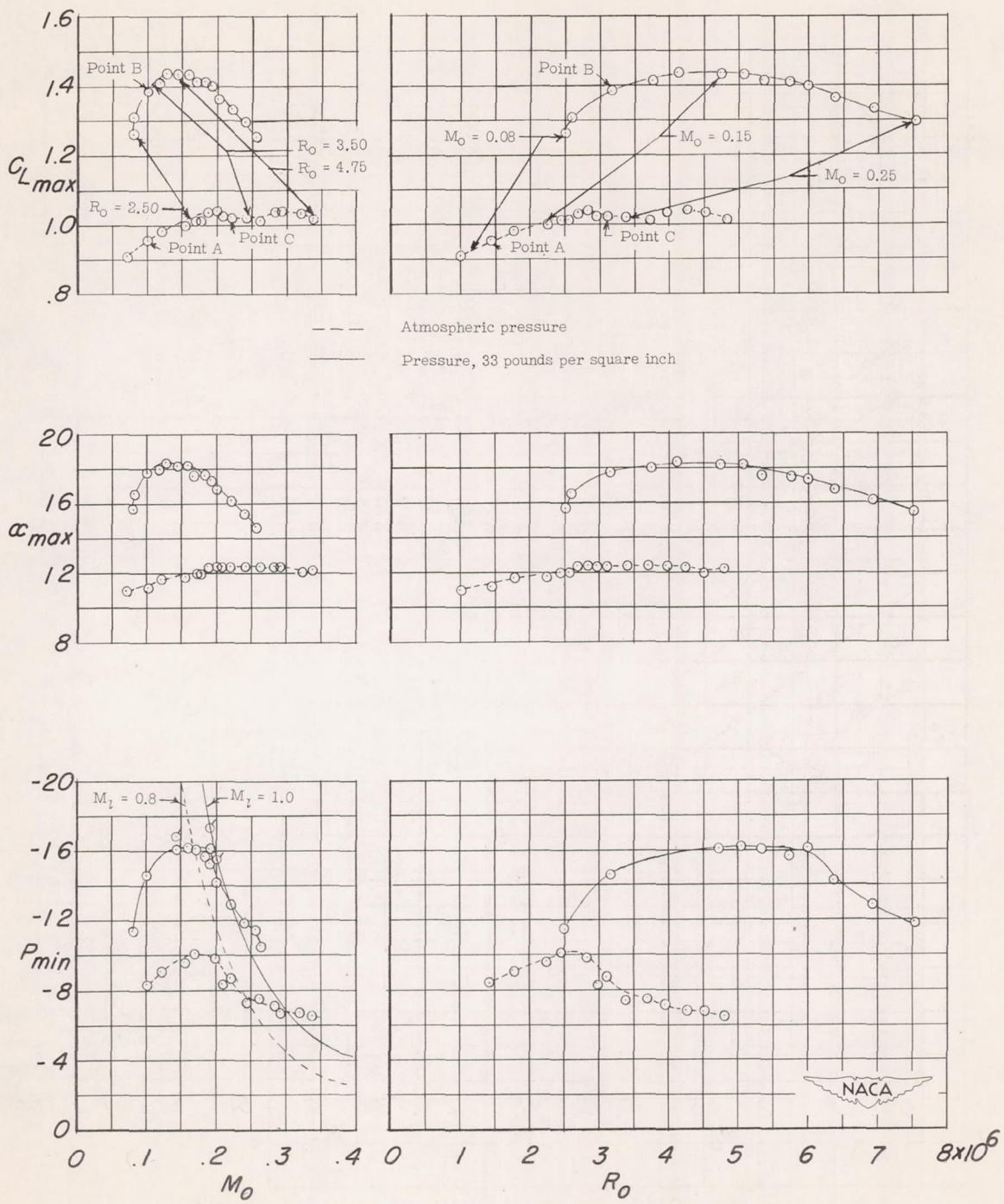
(a) Atmospheric pressure.

Figure 7.- Variation of lift coefficient with angle of attack for various Mach numbers and Reynolds numbers. Flagged symbols denote leading edge rough. 0.99-span split flaps deflected 60°.



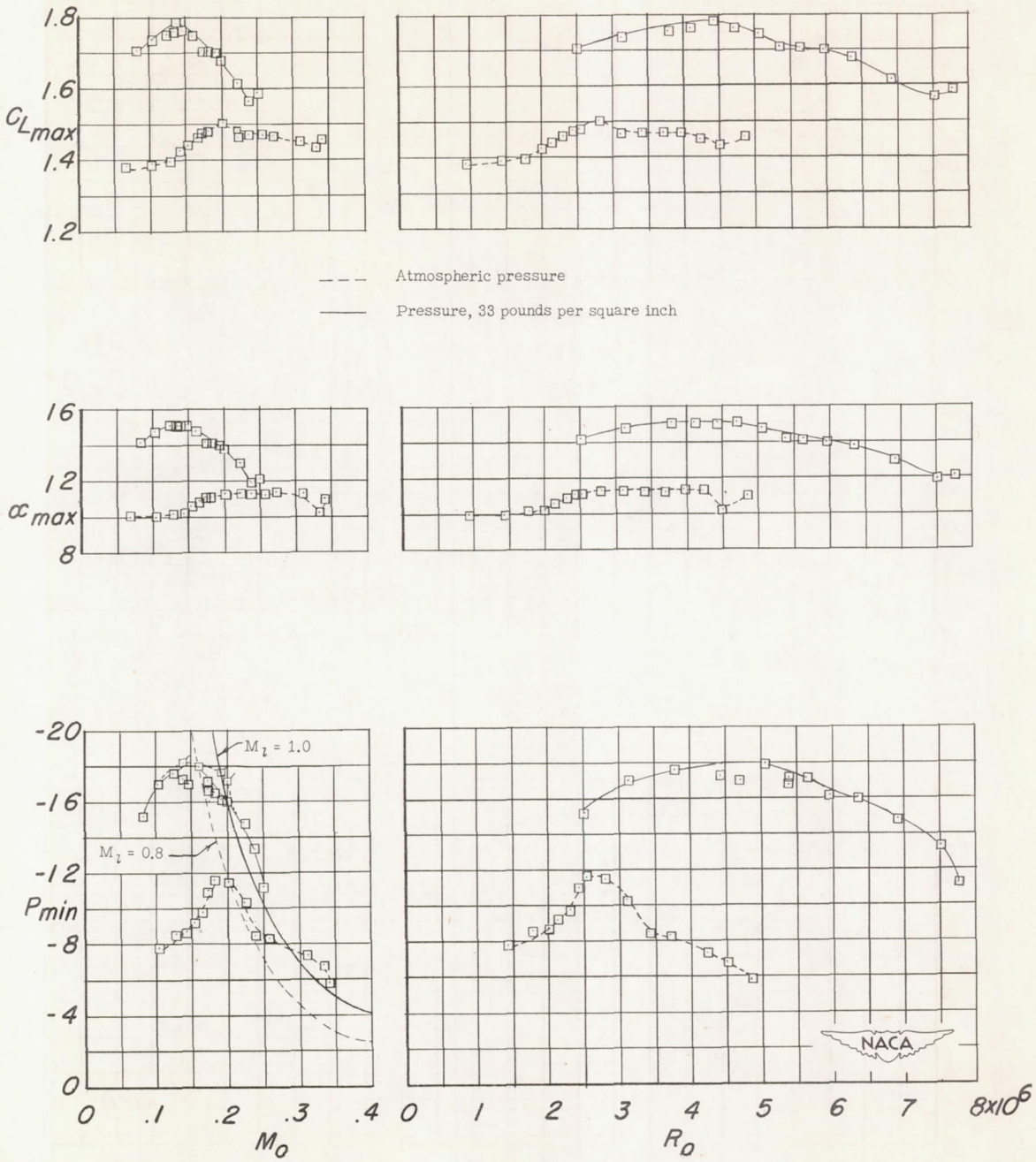
(b) Pressure, 33 pounds per square inch.

Figure 7.- Concluded.



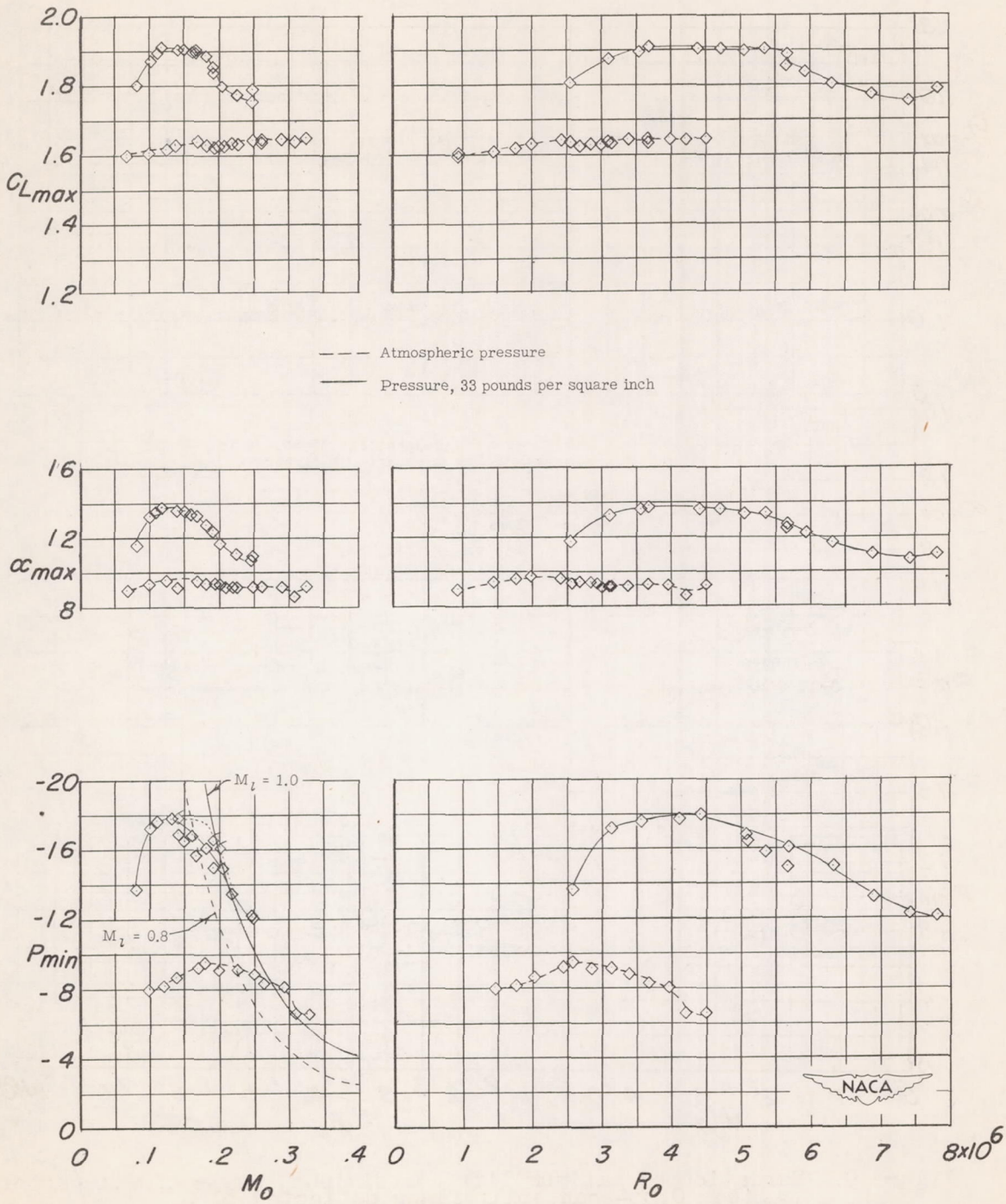
(a) Plain wing.

Figure 8.- Variation of maximum lift coefficient, angle of attack for maximum lift, and minimum pressure coefficient with Mach number and Reynolds number. Flagged symbols denote maximum of pressure fluctuation. Leading edge smooth.



(b) 0.55-span split flaps deflected 60°.

Figure 8.- Continued.



(c) 0.99-span split flaps deflected 60°.

Figure 8.- Concluded.

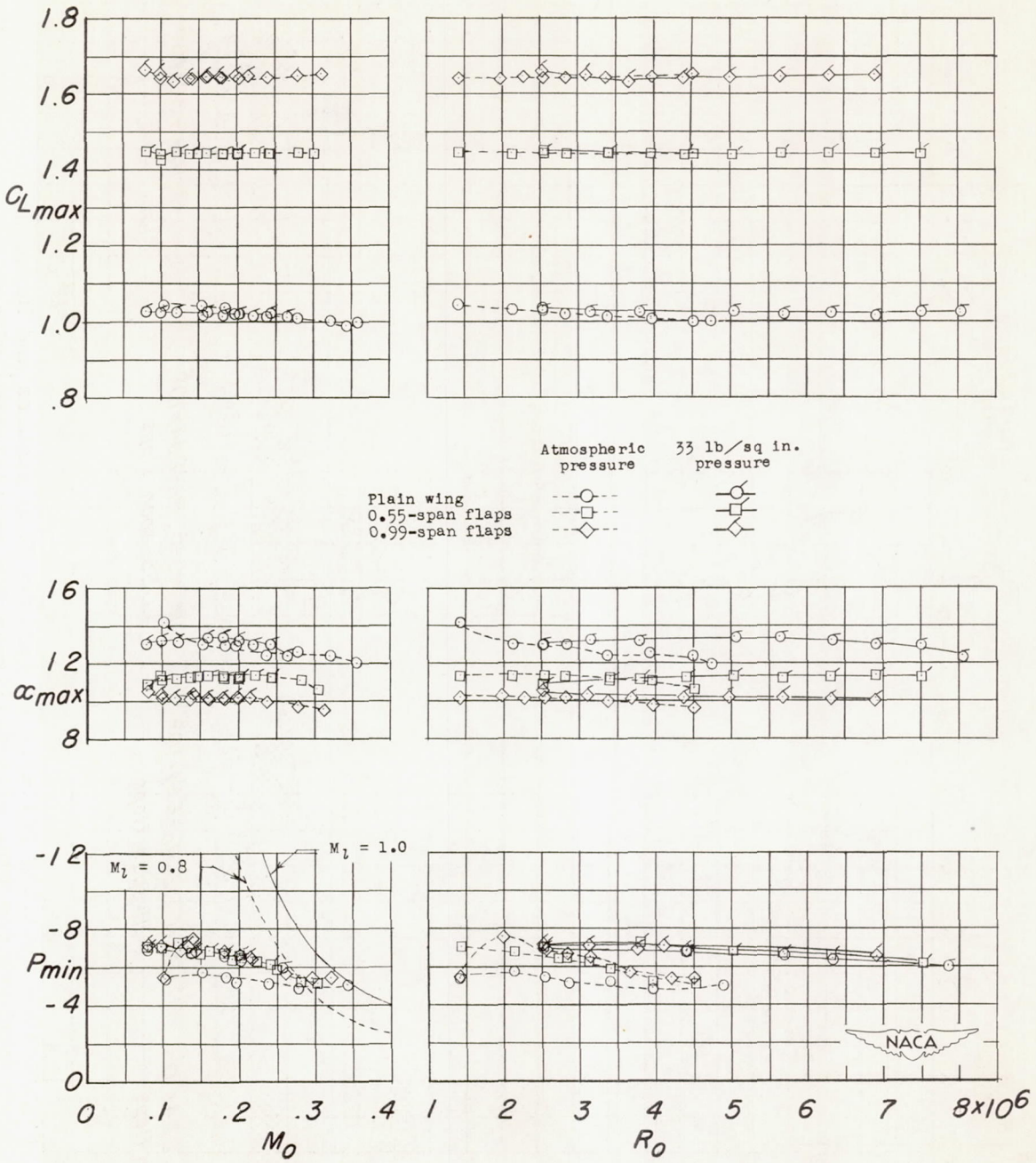


Figure 9.- Variation of maximum lift coefficient, angle of attack for maximum lift, and minimum pressure coefficient with Mach number and Reynolds number. Leading edge rough.

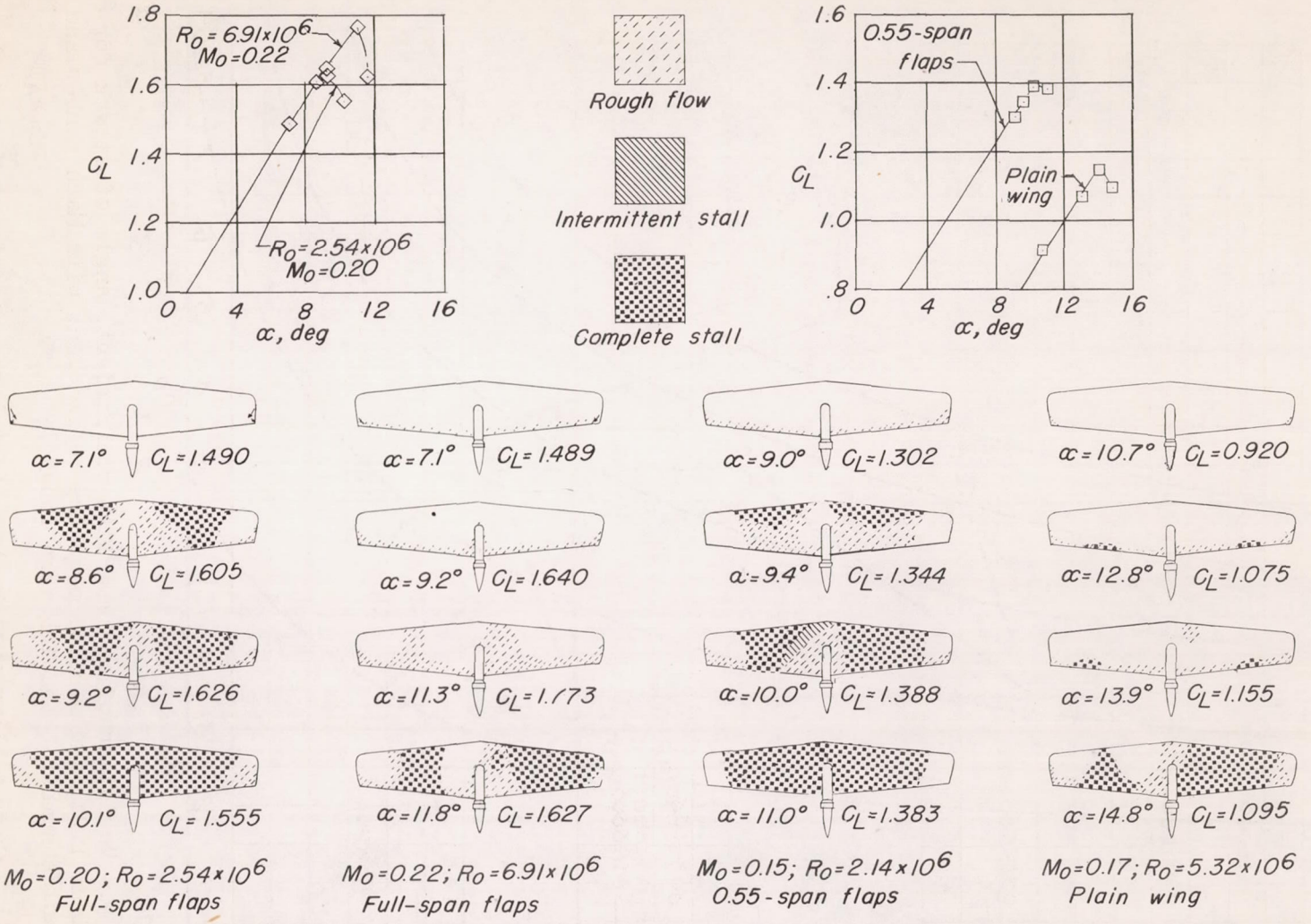


Figure 10.- Stalling patterns at various Mach numbers and Reynolds numbers for wing with full-span and partial-span flaps.

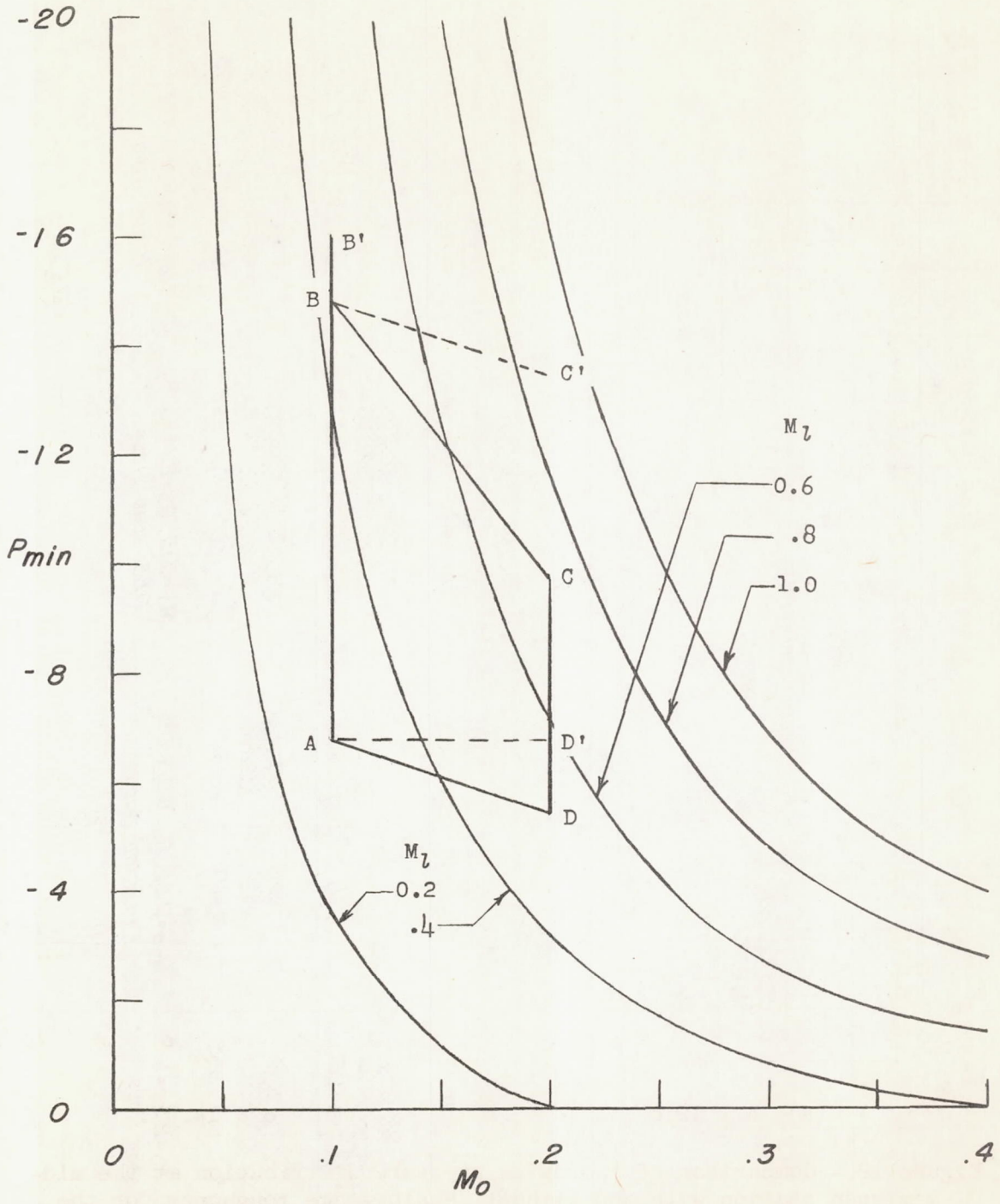
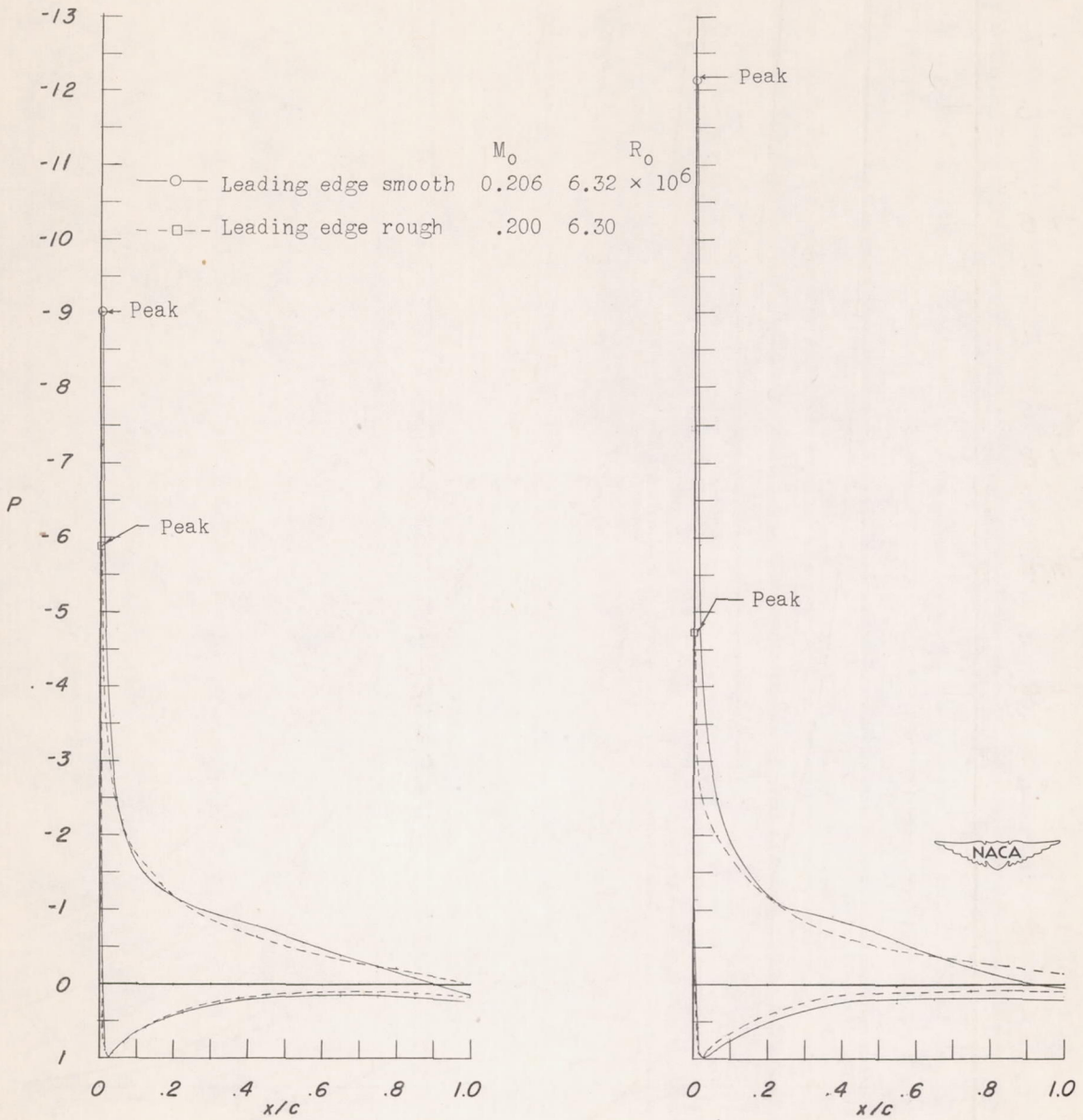
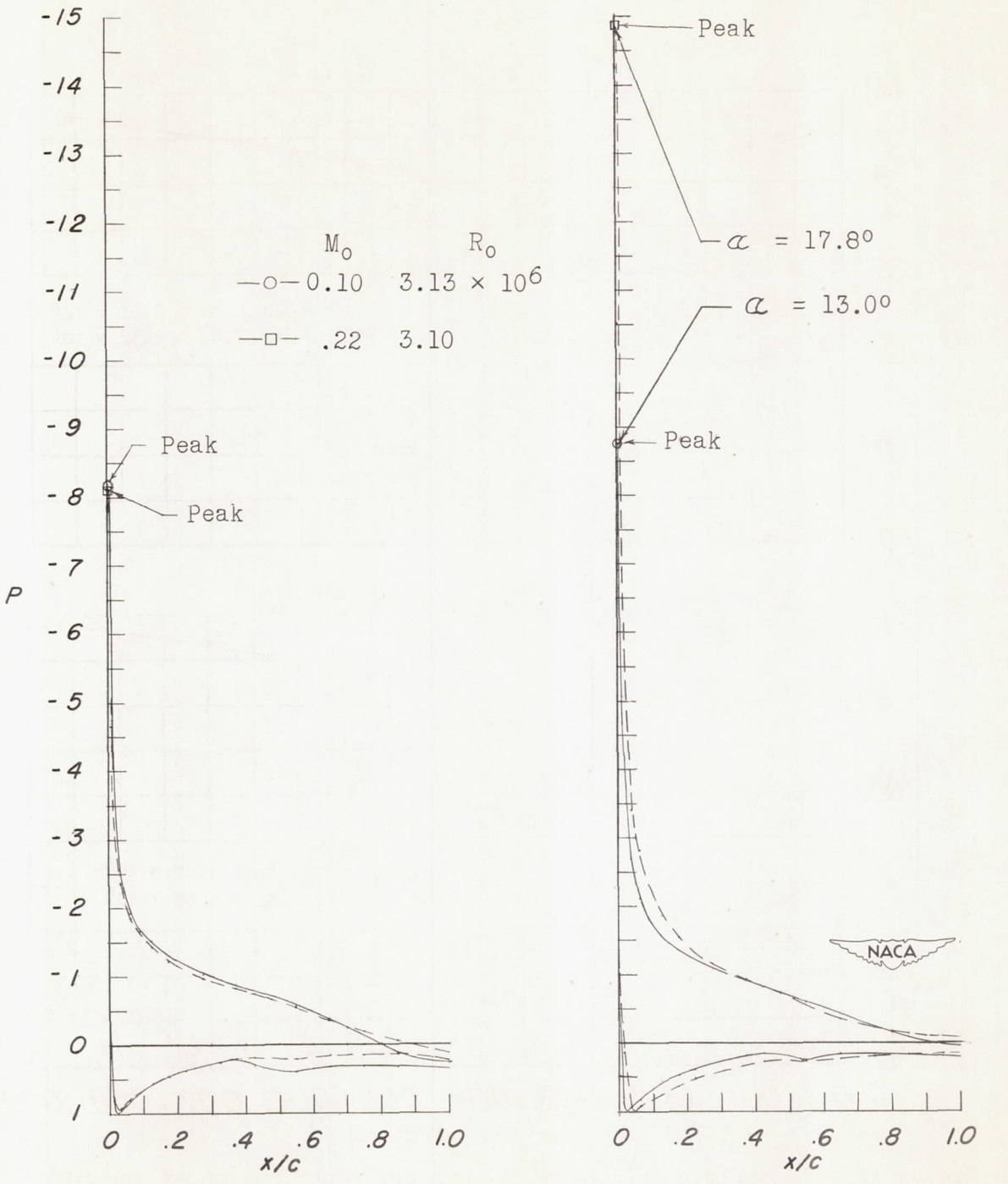


Figure 11.- Curves illustrating the interrelated effects of Mach number and Reynolds number.



(a) $\alpha = 12.8^{\circ}$. (b) $\alpha = 14.4^{\circ}$.

Figure 12.- Comparison of chordwise pressure distribution at the mid-semispan station with and without leading-edge roughness for the plain wing.



(a) $\alpha = 12.8^{\circ}$.

(b) $\alpha = \alpha_{max}$.

Figure 13.- Typical chordwise pressure distribution for the plain wing at different Mach numbers and approximately the same Reynolds number.

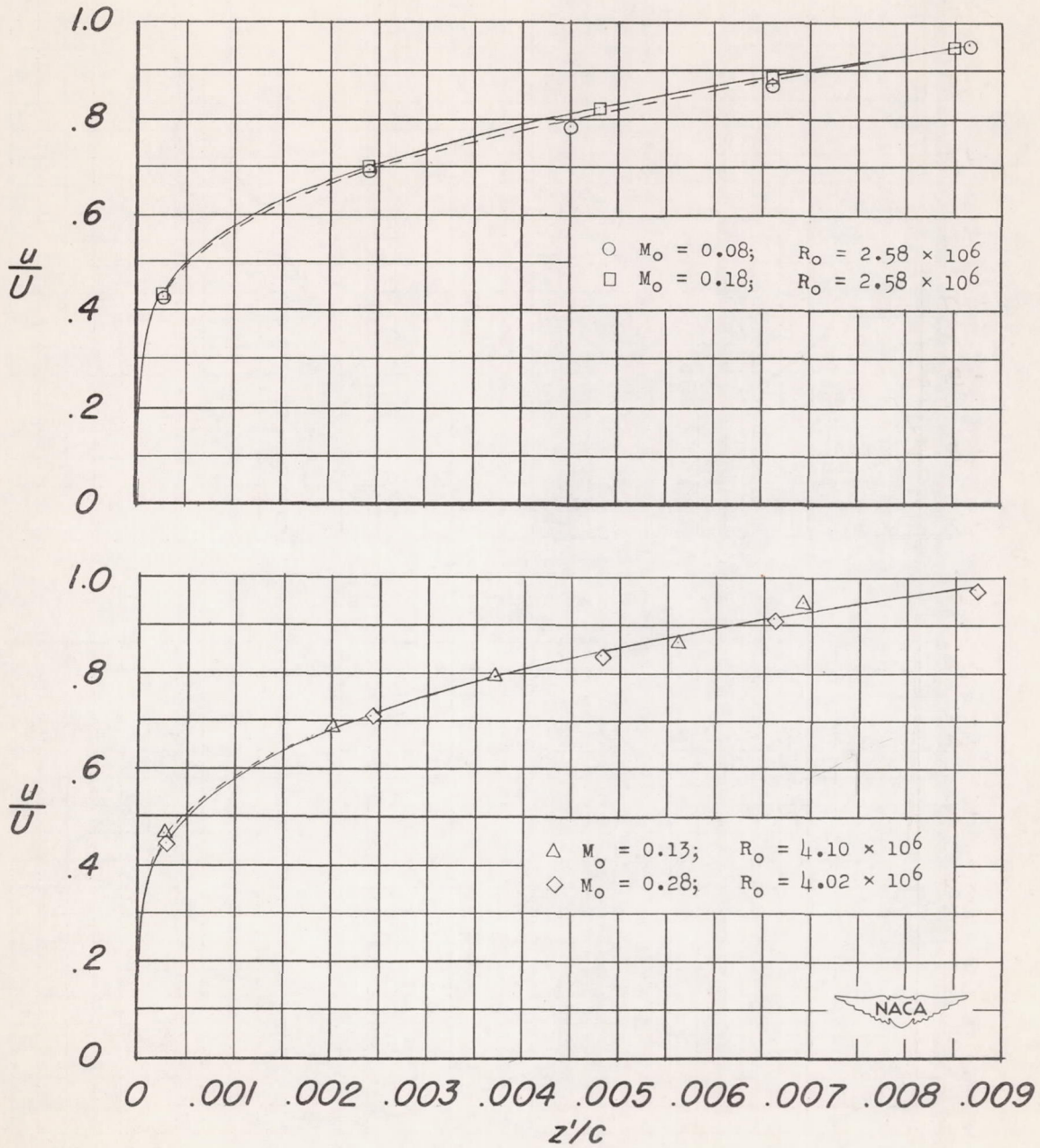
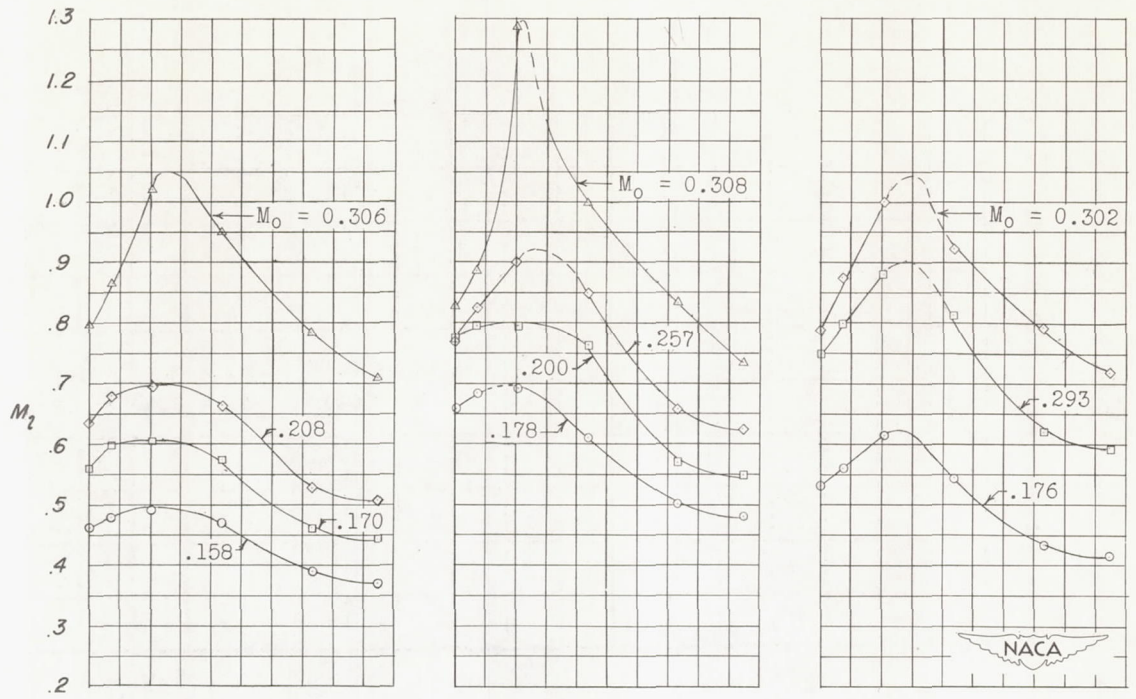
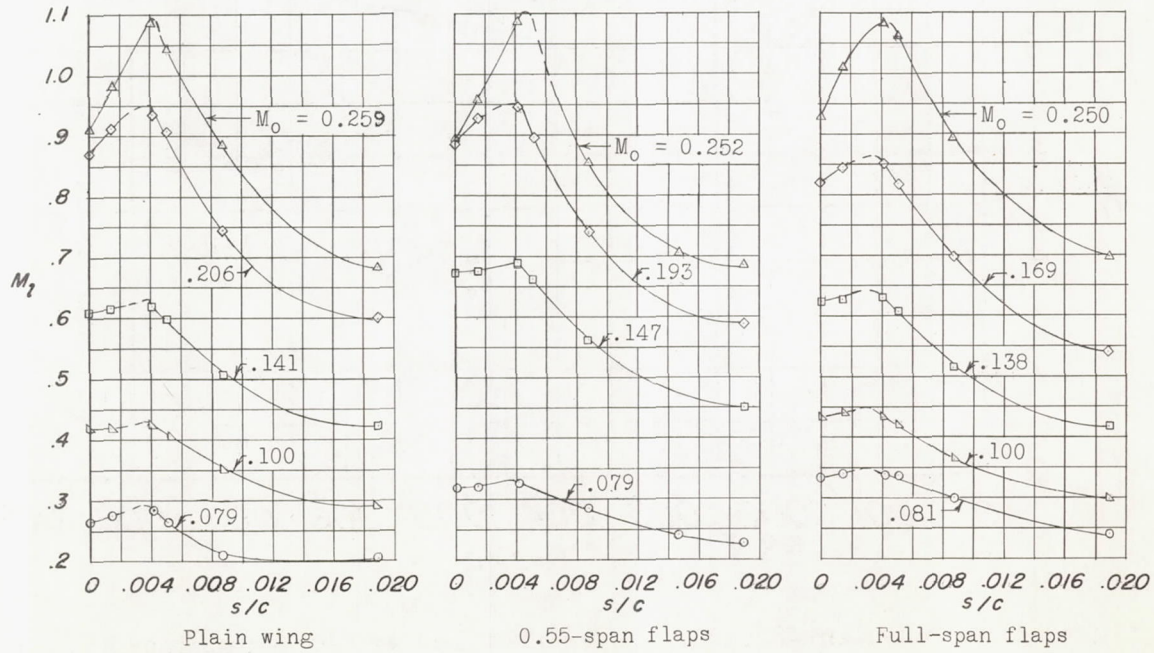


Figure 14.- Turbulent-boundary-layer profiles at the midsemispan station at x/c of 0.50. $\alpha = 6.5^\circ$.



(a) Atmospheric pressure.



(b) Pressure, 33 pounds per square inch.

Figure 15.- Variation of local Mach number with distance from the leading edge at maximum lift. Data obtained at midsemispan station.

NACA-Langley - 8-14-52 -1000